BIOCHEMISTRY
including biophysical chemistry & molecular biology

Article

pubs.acs.org/biochemistry

Mechanism of Copper Incorporation in Subunit II of Cytochrome *c* Oxidase from *Thermus thermophilus*: Identification of Intermediate Species

Manas Kumar Ghosh, Priyanka Basak, and Shyamalava Mazumdar*

Department of Chemical Sciences, Tata Institute of Fundamental Research, Colaba, Mumbai 400005, India

Supporting Information

ABSTRACT: Detailed spectroscopic and kinetic studies of incorporation of copper ion in the wild type (WT) and the D111AA (AA = K, N, or E) mutants of the metal ion binding site of the soluble fragment of subunit II of cytochrome *c* oxidase from *Thermus thermophilus* ($TtCu_A$) showed the formation of at least two distinct intermediates. The global analyses of the multiwavelength kinetic results suggested a four-step reaction scheme involving two distinct intermediates in the pathway of incorporation of copper ions into the apoprotein forming the purple dinuclear Cu_A. An early intermediate similar to the red copper binding proteins was detected in the WT as well as in all the mutants. The second intermediate was a green copper species in the case of WT $TtCu_A$. Mutation of Asp111, however, formed a second intermediate that is distinctly different from that formed in the case of the WT protein, suggesting that mutants follow pathways of copper ion incorporation different from that in the WT protein. The electrostatic interaction between Asp111 and the coordinating His114 possibly plays a subtle role in the mechanism of incorporation of metal ion into the protein. The overall K_d for WT $TtCu_A$ was found to be ~8 nM, which changed with mutation of the Asp111 residue. The activation and thermodynamic parameters were also determined from the temperature- and pH-dependent multiwavelength kinetics, and the results are discussed to unravel the role of Asp111 in the mechanism of formation of the dinuclear Cu_A center in cytochrome *c* oxidase.

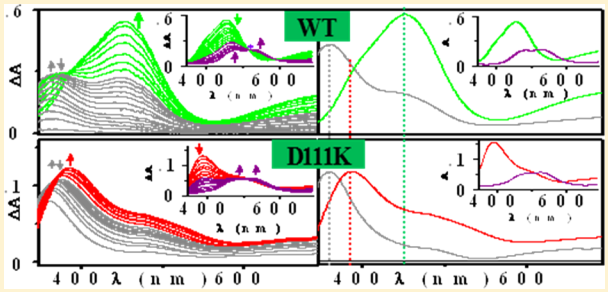

Cytochrome *c* oxidase (CcO) is the terminal respiratory enzyme, which belongs to a heme copper oxidase superfamily. The purple dinuclear copper center (Cu_A) forms the electron entry site in CcO.[1] The structure of the Cu_A site is found to be highly conserved in subunit II of cytochrome *c* oxidases of eukaryotic mitochondria[2] and aerobic bacteria[3−6] and in the nitrous oxide reductase (N_2OR) of denitrifying bacteria.[7,8] Existing at a solvent-exposed part of subunit II of the enzyme, the Cu_A site accepts the electrons from cytochrome *c* and subsequently transfers the electrons via the six-coordinated heme center to the heteronuclear heme a_3−Cu_B catalytic center in subunit I of the enzyme for reduction of molecular oxygen to water.[9] The Cu_A site of the ba_3 oxidase from *Thermus thermophilus* consists of 10 antiparallel β-sheets forming a β-barrel fold in a cupredoxin topology, which was proposed to have a significant effect in adopting the novel coordination geometry of the dicopper center.[10,11] The solvent-exposed fragment consisting of 124 residues containing the intact purple Cu_A site ($TtCu_A$) of ba_3 oxidase was obtained by cleaving the first 44 amino acids of subunit II of CcO.

The crystal structure [Protein Data Bank (PDB) entry 2CuA (Figure 1)] shows that two cysteine residues (C149 and C153) bridge a pair of Cu atoms with a short Cu−Cu distance of 2.4−2.5 Å.[4,12] One of the copper ions (Cu1) is coordinated to H157 and Q151, while the other copper ion (Cu2) is bound to H114 and M160. These residues are invariant in all homologues of the enzyme (Figure S1 of the Supporting Information), except Q151 in $TtCu_A$ corresponds to a Glu residue (E247) bound to Cu_A in the aa_3 oxidase from *Paracoccus denitrificans* that is also coordinated to the Mn center at the interface between the two subunits. Residues 149−160 forming a hairpin loop (L1) between β-sheets 9 and 10 and one histidine residue (H114) from the hairpin loop (L2) between sheets 5 and 6 in the protein form the binding site of the dinuclear copper center in $TtCu_A$ (Figure 1). The crystal structure further indicates that the aspartic acid residue (D111) is hydrogen bonded (2.8 Å) to H114 that is coordinated to one of the copper ions.[4,13] Analyses of the sequence homology among forms of CcO from bacterial and mammalian sources showed that the D111 residue (in L2) is invariant in the homologous proteins (Figure S1 of the Supporting Information). It is thus important to understand the specific role of the D111 residue in the formation and stability of the purple dinuclear Cu_A center of the protein.

The formation of the intact Cu_A center by assembly of two copper ions to the protein *in vivo* is a complex process, which has been proposed to involve one or more copper chaperones.[14−17] The assembly of the Cu_A center of subunit II of CcO of *Bacillus subtilis* was shown to involve Cu(II)-bound

Received: January 26, 2013
Revised: May 11, 2013
Published: June 7, 2013

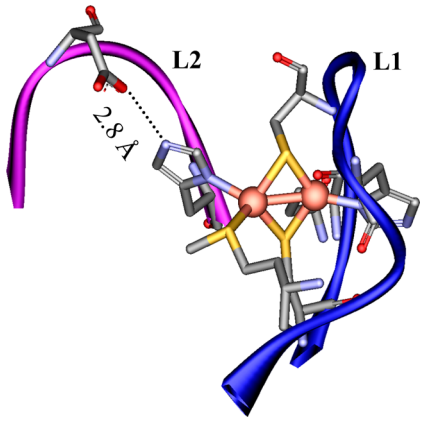

Figure 1. Schematic structure of $TtCu_A$ (PDB entry 2CuA) showing Asp111 in the copper ion binding loops and the coordinating residues to the binuclear copper center. The copper binding loops are colored blue (L1) and magenta (L2). The dotted line shows the proposed hydrogen bonding between Asp111 and His114. Spheres indicate the copper ions.

Sco.[14] On the other hand, nuclear magnetic resonance studies indicated that Cu(I)-bound PCu_AC transfers the metal ion to the apoprotein of $TtCu_A$, while the reduced form of Sco helps in regeneration of the disulfide form of apo-$TtCu_A$.[16] None of these reports, however, provided any mechanistic insight into the assembly of the dinuclar Cu_A center of the protein. Studies of the *in vitro* formation of the purple Cu_A center of the chimeric Cu_A protein derived from azurin (Cu_AAz), the Cu_A center of N_2OR, and that of $TtCu_A$[15,18−20] using $CuSO_4$ proposed the formation of mononuclear intermediate species. Although the residues in the first coordination sphere of Cu_A are expected to be important for the formation of the intact metal center, the role of the outer coordination sphere is not yet known. It is also important to note that the *in vivo* assembly of the metal center would involve ligand exchange reactions between the chaperone and the apoprotein of Cu_A. Both Sco and PCu_AC have been shown to bind copper ion through one or more His residues. Thus, $Cu(His)_2$ would possibly be better than $CuSO_4$ for *in vitro* modeling of incorporation of copper ion into the apoprotein of Cu_A.

To improve our understanding of whether the outer sphere interaction involving the hydrogen bonding between H114 and D111 in the $TtCu_A$ could play any role in the metal ion incorporation pathway, we have studied the kinetics of the reaction of $Cu(His)_2$ with the WT and the D111AA (AA = K, N, or E) mutants of apo-$TtCu_A$ at different temperatures and pHs. These studies highlighted the kinetic and thermodynamic contributions of Asp111 to the formation of the purple dinuclear center. Our results show that the uptake of copper by the apoprotein is a multistep process as reported previously,[18−20] and two distinct intermediate species were detected. The early intermediate was similar to that reported to be formed in the case of several other copper binding proteins.[15,21−24] The second intermediate of the WT protein agreed with the green intermediate reported recently.[15] Although the early intermediate was spectroscopically the same in the mutant proteins as observed in the case of the WT protein, the mutation of Asp111 gave rise to a spectroscopically different second intermediate species that was similar to the previously reported red copper sites in nitrosocyanin.[25,26]

MATERIALS AND METHODS

Materials and Reagents. Bactotryptone and yeast extract were purchased from HiMedia. Restriction enzymes and buffers for molecular biology were purchased from New England Biolabs. QuikChange site-directed mutagenesis kits were purchased from Stratagene. The primers were purchased from Sigma Chemicals. DTNB was purchased from Sigma Chemicals. The CM-Sepharose column was purchased from GE Healthcare. The dialysis membrane was purchased from Spectra/Por Thomas Scientific, USA. General reagents were obtained from Sigma.

Mutation, Expression, and Purification. The wild-type $TtCu_A$ gene from *T. thermophilus* was inserted between NcoI and BamHI restriction sites in the pMA10 vector[10] obtained from B. Ludwig. Site-directed mutagenesis was conducted using the QuikChange site-directed mutagenesis kit from Agilent Technologies Inc. The forward primers used for the mutation of aspartic acid 111 to lysine, asparagine, and glutamic acid were 5′-GATCACGAGCCCGaaaGTGATCCACGGC-3′, 5′-GATCACGAGCCCGaacGTGATCCACGGC-3′, and 5′-CA-AGATCACGAGCCCGgaaGTGATCCAC-3′, respectively, and the corresponding reverse primers were 5′-GCCGTGGATC-ACtttCGGGCTCGTGATC-3′, 5′-GCCGTGGATCACgttCG-GGCTCGTGATC-3′, and 5′-GTGGATCACttcCGGGCTC-GTGATCTTG-3′, respectively. These primers removed BtrI restriction sites from the $TtCu_A$ gene along with D111K, D111N, and D111E mutations (shown in lowercase letters), respectively. Polymerase chain reaction (PCR) was performed to amplify the mutant gene on a PTC-2000 Peltier thermocycler (MJ Research, Waltham, MA). Mutations were confirmed by restriction enzyme digestion as well as by DNA sequencing. The WT and D111AA mutant plasmids were freshly transformed in BL21(DE3) cells. Expression of the protein was conducted using the reported method.[27,28] One single colony was inoculated and grown overnight in 100 mL of Luria-Bertani (LB) medium containing 100 μg/mL ampicillin at 37 °C by being shaken at 170 rpm; 5% inoculums were used to inoculate 1 L of LB medium containing 100 μg/mL ampicillin. The culture was induced with 0.4 mM IPTG (isopropyl β-D-thiogalactopyranoside) at an OD_{600} of 0.6. The resultant culture was grown for 6 h at 37 °C and 150 rpm. The bacterial cells were harvested by centrifugation at 5000 rpm for 20 min at 4 °C. The cells were resuspended in 10 mL of lysis buffer [50 mM Tris-HCl (pH 8), 0.1 mg/mL lysozyme, 1 mM DTT, 5 mM PMSF, 2 μg/mL leupeptin, 2 μg/mL pepstatin, 2 μg/mL aprotinin, 40 units/mL DNase, and 10 mM $MgCl_2$] and stirred at 4 °C for 30 min. The cells were lysed for 1 h using a sonicator (Hielscher ultrasound technology) at 30 pulses/min. The supernatant was collected after centrifugation at 17000 rpm for 90 min at 4 °C, and the pH was adjusted to 4 with 500 mM sodium acetate (NaOAc), resulting in a significant precipitation. The mixture was centrifuged at 17000 rpm for 30 min at 4 °C, and the supernatant was loaded onto a CM-Sepharose column, pre-equilibrated with 50 mM NaOAc (pH 4) and subjected to a step gradient with 1 M sodium chloride (NaCl). The desired apoprotein of $TtCu_A$ was eluted at 31−43% salt, which was found to be ∼95% pure as characterized by a single band via sodium dodecyl sulfate−polyacrylamide gel electrophoresis. The eluted protein was concentrated in a 15 mL centrifugal filter unit with a 10 kDa molecular mass cutoff (Amicon Ultra, Millipore). The purified protein was stored at −20 °C in 20% glycerol, and aliquots of the protein were dialyzed using an 8 kDa dialysis membrane (Spectra/Por Thomas Scientific, USA) to remove

dx.doi.org/10.1021/bi400101g | *Biochemistry* 2013, 52, 4620−4635

glycerol prior to every experiment. Protein concentrations were determined by using the Bradford assay.[29] The yields of the apoprotein of the WT and mutants were found to be ~4 mg/L of culture medium.

Thiol Assays. Thiol assays were performed on the apoprotein of both the WT and the D111AA (AA = K, N, or E) mutants of $TtCu_A$ in 100 mM sodium phosphate buffer (pH 7) containing 1 mM EDTA (ethylenediaminetetraacetic acid). The protein concentration was 3 μM for the WT and all three mutants. The thiol content of the apoprotein was estimated by a reported method.[30,31] The thiol reactive reagent DTNB [5,5′-dithiobis(2-nitrobenzoic acid)] was added to a final concentration of 300 μM. The number of free thiols per molecule of apoprotein was determined by determining the number of TNB (2-nitro-5-thiobenzoic acid) anions released upon reaction with the free thiol. The absorbance change was followed at 412 nm, and an extinction coefficient of 14150 M^{-1} cm^{-1} was used for TNB anion.[30,31]

UV−Visible Spectroscopy. UV−visible absorption spectra were measured on a Perkin-Elmer Lambda 750 UV−vis spectrophotometer coupled with a Peltier-controlled thermostated cell holder. The optical absorption was monitored between 250 and 800 nm.

Circular Dichroism Spectroscopy. Circular dichroism (CD) spectra were recorded on a JASCO J-810 spectropolarimeter equipped with a Peltier cell temperature controller. The CD spectra were recorded from 240 to 200 nm in a 0.1 cm path length quartz cell cuvette for the far-UV region. The CD parameters were as follows: scan speed of 20 nm/min, time constant of 1.0 s, bandwidth of 1.0, and sensitivity of 100 mdeg. All experiments were conducted under a flow of pure nitrogen. A good signal-to-noise ratio in the CD spectra in this spectral range was obtained on data averaging over three scans. Protein solutions (12 μM) were used for far-UV CD studies. The CD spectra in the far-UV region (240−200 nm) were analyzed using Reed's method to estimate the secondary structure of the protein.[32]

Thermal Unfolding. The temperature dependence of the far-UV CD was monitored to determine the thermal unfolding of the secondary structures of the WT and the D111AA mutants of $TtCu_A$. The temperature of the sample was increased from 20 to 90 °C at a heating rate of 1 °C/min. The samples were equilibrated for at least 3 min at each temperature, and the reversibility of the unfolding was ensured by decreasing the temperature with a cooling rate of 1 °C/min.

The thermal unfolding data, monitored at different wavelengths, were analyzed using a two-state equilibrium model between native (N) and unfolded (U) conformations (N ⇋ U). The data were fit to the following sigmoid function derived from the temperature dependence of the unfolding equilibrium constant by a small approximation in the Gibbs−Helmhohltz equation[33] ($1/RT \approx 1/RT_m$ and $T/T_m \approx 1$ in this case) to obtain the melting temperature (T_m) of the apoprotein of the D111K mutant.

$$\theta_{obs} = \frac{\theta_N + \theta_U e^{B(1-T/T_m)}}{1 + e^{B(1-T/T_m)}} \quad (1)$$

where θ_{obs} is the observed ellipticity at a given wavelength and temperature, θ_N and θ_U are the ellipticities at a given wavelength for the folded and unfolded forms of the protein, respectively, and B is a constant parameter, which is a function of the thermodynamic constants (ΔH_m and ΔC_p) at the midpoint temperature (T_m).

Stopped-Flow UV−Visible Absorption Kinetics. Experiments were conducted using a thermostated Hi-Tech Scientific SF-61 MX2 stopped-flow multi-mixing spectrofluorimeter equipped with a 96-element photodiode array detector. Two-syringe mixing was employed to mix equal volumes of the WT $TtCu_A$ apoprotein or D111AA mutants (0.18 mM) with varied concentrations of a $Cu(His)_2$ solution (0.5−2 mM) at different pHs in universal buffer (UB) containing metal free 50 mM MES, MOPS, Tris, CAPS, and NaOAc. The sampling unit was mounted inside a thermostated bath compartment with a varying temperature (within ±1 °C) using a circulating water bath. The solutions were mixed in the stopped-flow apparatus, and the time-dependent absorption change was monitored using a diode array system. The integration period was 1 ms. All data sets originally consisted of 96 spectra collected over two time windows. The temperature-dependent metal incorporation kinetics was monitored at different constant temperatures between 10 and 30 °C only at ambient pH (pH 7).

Global Analyses of Stopped-Flow UV−Visible Absorption Kinetics Data. Kinetics data were analyzed using Pro-K (Applied Photophysics Limited), which employed singular-value decomposition (SVD) and nonlinear regression modeling to estimate the kinetic parameters from the data. Pro-K allows global analysis of the complete data set according to the proposed reaction model, providing a best fit parameter set that accommodates all kinetic behavior across the entire measured wavelength range.[34,35]

Freeze Quenching of the Reaction Mixture at Different Time Intervals. Freeze quenching of the reaction mixture of the apoprotein with $Cu(His)_2$ at a short time interval was conducted at pH 7 using a Bio-Logic science SFM 400 instrument with an MPS-60 microprocessor unit in quench-flow mode. The sample containing mixtures of transient intermediates was prepared by mixing 0.428 mM WT $TtCu_A$ apoprotein with 0.171 mM $Cu(His)_2$ in 50 mM Tris buffer [tris(hydroxymethyl)aminomethane] containing 20% glycerol at 25 °C, and the reaction mixture was passed through a delay line to achieve a mixing time of 250 ms. The sample was flash-frozen by being collected in an electron paramagnetic resonance (EPR) sample tube, precooled to approximately −150 °C using an isopentane bath dipped into a liquid nitrogen container. The sample was kept at −80 °C for the EPR experiment.

Electron Paramagnetic Resonance Spectroscopy. The X-band EPR spectra were recorded at 93.7 K (liquid N_2) on a Bruker EMX microspectrometer with a microwave frequency of 9.26 GHz along with a continuous flow of nitrogen cryostat. The temperature accuracy of the instrument is ±1 K; 20% glycerol was used as a glassing agent. X-Band EPR experimental conditions were as follows: microwave power of 2 mW, modulation amplitude of 2 G, time constant of 1.3 s, and conversion time of 98 ms.

Data Analysis. The time course of $TtCu_A$ metal incorporation (Scheme 1) was analyzed in each time window using Pro-K to determine the pseudo-first-order rate constant (k_{obs}). The observed rate constant (k_{obs}) was plotted as a function of Cu(II) concentration to estimate the off rate (k_{off}) constants of the copper-bound protein. The apparent forward rate constant (k_{app}) was obtained from the differences between the k_{obs} and k_{off} values. The logarithm of k_{app} was plotted as a function of the logarithm of Cu(II) concentration to determine

dx.doi.org/10.1021/bi400101g | Biochemistry 2013, 52, 4620−4635

Scheme 1. Proposed Reaction Steps Involved in Copper Incorporation in $TtCu_A$[a]

[STEP 1]: Cu(II) + A[HS] → X [Cu(II)]

[STEP 2]: Cu(II) + X[Cu(II)] → Y [Cu_2(II)], Z [Cu_2(II)], W [Cu_2(II)] or V [Cu_2(II)]

[STEP 3]: 2Cu(II) + A[HS] → 2Cu(I) + A' [S-S] +$2H^+$

[STEP 4]: Cu(I) +Y [Cu_2(II)], Z [Cu_2(II)], W [Cu_2(II)] or V [Cu_2(II)] → H[Cu(II), Cu(I) or Cu_2(1.5)]

[a]X[Cu(II)] is first intermediate for the WT and the D111AA (AA = K, N, or E) mutants at pH 5−7. Y[Cu_2(II)] is the second intermediate for WT at pH 5−7. Z[Cu_2(II)], W[Cu_2(II)], and V[Cu_2(II)] are second intermediates for D111AA mutants at pH 7, 6, and 5, respectively. H[Cu(II), Cu(I)], or H[Cu_2(1.5)] is a holoprotein for the WT and the D111AA mutants at pH 5−7. A[HS] and A′[S−S] are the reduced and oxidized apoprotein, respectively.

the order of the reaction from the slope and bimolecular rate constants (k_{on}) from the corresponding intercepts of the plots.

The logarithm of k_{on} was plotted as a function of the reciprocal of the absolute temperature (T) to determine the energy of activation (E_a) of the proteins by the Arrhenius equation (eq 2), where A is the pre-exponential factor.

$$\ln(k_{on}) = -\frac{E_a}{RT} + \ln(A) \quad (2)$$

The thermodynamic parameters of activation such as activation enthalpy ($\Delta H^{\ddagger}$), activation entropy ($\Delta S^{\ddagger}$), and free energy of activation ($\Delta G^{\ddagger}$) were determined by the Eyring equation (eqs 3 and 4) from the plot of the logarithm of k_{on}/T as a function of $1/T$.[27]

$$\ln \frac{k_{on}}{T} = -\frac{\Delta H^{\ddagger}}{RT} + \frac{\Delta S\ddagger}{R} + \ln \frac{k_B}{h} \quad (3)$$

$$\Delta G^{\ddagger} = \Delta H^{\ddagger} - T\Delta S^{\ddagger} \quad (4)$$

where R is the universal gas constant and k_B and h are Boltzmann's and Planck's constants, respectively.

The equilibrium free energy (ΔG^{Eq}) was obtained from eqs 5 and 6.

$$K_d = \frac{k_{off}}{k_{on}} \quad (5)$$

where K_d is the dissociation constant.

$$\Delta G^{Eq} = RT \ln K_d \quad (6)$$

RESULTS AND DISCUSSION

The UV−visible absorption spectra of the apoprotein of the WT and D111AA (AA = N, K, or E) mutants of $TtCu_A$ showed a characteristic peak at 280 nm. The absence of any peaks in the visible region confirmed that there was no holoprotein present in the solution (data not shown). The characteristic peaks at 360, 480, 530, and 790 nm of the holoprotein of $TtCu_A$ with an intense purple color were observed upon addition of $Cu(His)_2$ to the apoprotein (data not shown).

To identify whether the mutation of the protein had any effect on the secondary structure of the protein, we have studied the CD spectra of the WT and D111AA mutants of $TtCu_A$ at different pHs. The secondary structural elements such as α-helix, β-sheet, turn, and random coil were estimated using Reed's method,[32] and the results are listed in Table S4 of the Supporting Information. The far-UV CD spectra of the apoprotein of the WT and D111AA mutants of $TtCu_A$ are shown in Figure S11 of the Supporting Information. The results showed that the apoproteins of WT, D111N, D111K, and D111E $TtCu_A$ show small variations in the far-UV CD spectra at pH 5, suggesting that the secondary structure of $TtCu_A$ was slightly affected (Figure S11 and Table S4 of the Supporting Information) upon mutation of Asp111.

The thermal stabilities of the apoprotein of the WT and the D111AA mutants of $TtCu_A$ were investigated using temperature-dependent far-UV CD spectroscopy at multiple wavelengths. The results showed that the β-barrel fold in the apoproteins of WT, D111N, and D111E $TtCu_A$ is stable up to 90 °C at pH 5 (Table S4 of the Supporting Information). This indicated that the hydrogen bonding between the H114 and the residue at position 111 (i.e., Asp in the WT protein and Asn or Glu in the mutants) is possibly still intact upon mutation of Asp111 in D111N and D111E. On the other hand, the thermal stability of the β-barrel fold in the apoprotein of the D111K mutant of $TtCu_A$ seems to be drastically lower than that of the WT protein at pH 5 (Table S4 and Figure S12 of the Supporting Information), with a midpoint temperature 67 °C possibly caused by destabilization of the secondary structure by the cationic residue (lysine) in place of Asp111. The results thus indicate that the hydrogen bonding between the NH group of H114 and the terminal C═O group of Asp111 (or Asn111 or Glu111 in the mutants) plays an important role in the thermostability of the apoprotein.

Kinetics of Incorporation of the Copper Ion into the Apoprotein of WT $TtCu_A$. Detailed studies of the kinetics of incorporation of copper ion into the apoproteins were conducted using the diode array detector in the stopped-flow setup so that snapshots of the spectral changes during the formation of the Cu_A center could be monitored. Equal volumes of the apoprotein (0.18 mM) were mixed with different concentrations (0.5−2 mM) of $Cu(His)_2$ solutions at different pHs and temperatures in the stopped-flow setup, and the spectral changes were collected using the diode array spectrometer. The reaction was found to have two distinct time scales, one in a faster time range involving formation of the intermediate(s) and the second on a longer time scale involving the formation of the purple copper center. The time-dependent absorption spectra were hence collected over two time windows, viz., T1 (shorter time) and T2 (longer time), to obtain well-resolved spectra.

The results show that there was an increase in absorbance at ∼370 and ∼455 nm within 3.7 ms of mixing of the solutions of the WT $TtCu_A$ apoprotein with $Cu(His)_2$. The peak at ∼370 nm subsequently decayed with a further increase in absorbance at ∼455 nm, which could be resolved in shorter time window T1 (0−240 ms with a time resolution of ∼2.5 ms) as shown in Figure 2A for WT $TtCu_A$ (Figure S2 of the Supporting Information shows results at different pHs). The formation of intermediate species X and Y with absorption peaks at ∼370 and ∼455 nm, respectively, was indicated in the results obtained in the short time window (T1) in the case of WT $TtCu_A$. However, in longer time window T2 (0−130 s with a time resolution of ∼1.35 s), the time resolution was much

dx.doi.org/10.1021/bi400101g | Biochemistry 2013, 52, 4620−4635

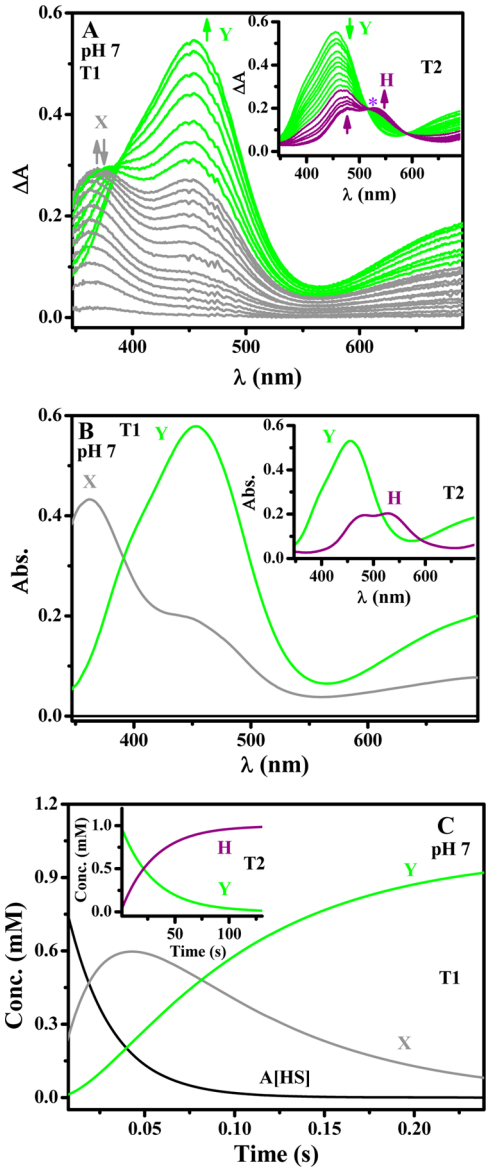

Figure 2. Stopped-flow UV−visible absorption spectra, resolved species spectra, and corresponding concentration profiles obtained from global analysis after 5.6 equiv of $Cu(His)_2$ had been mixed with the WT $TtCu_A$ apoprotein over T1 and T2 (inset) at pH 7 (A−C) in UB under aerobic conditions. The constant temperature of 15 °C was maintained during the time course of the reaction. The first spectrum was collected at 3.7 ms and 1.3 s (inset). Spectra are colored to correspond to the species forming in that particular time frame. Arrows indicate the direction of change in absorbance during the course of the experiment and are colored to correspond to the species forming in that time interval. The violet asterisk indicates the position of the apparent isosbestic point. A[HS] is the reduced apoprotein. H is the purple Cu_A. X and Y are intermediate species.

lower, and only the decay of the species corresponding to the peak at ∼455 nm (species Y, which was formed in the shorter time window) was observed with consequent formation of the characteristic spectra of the purple Cu_A (species H),[10,27,36] shown in the inset of Figure 2A (Figure S2 of the Supporting Information shows the results at different pHs). An isosbestic point at 515 nm was observed during the conversion of species Y to species H.

Analyses of the spectral profiles by Pro-K were conducted separately at each of the two time windows. The singular-value decomposition (SVD) analyses of the spectral profiles showed that there are three significant components (species) in the data obtained in time window T1 and two significant components (species) in time window T2. The spectra of the individual components (species) obtained for time windows T1 and T2 from the global analyses of the kinetic data using Pro-K are shown in Figure 2B and the inset, respectively (see Figure S2 of the Supporting Information for results for WT $TtCu_A$ at different pHs). The corresponding concentration profiles of the resolved components (species) are shown in Figure 2C and the inset, respectively (Figure S2 of the Supporting Information shows results for WT $TtCu_A$ at different pHs).

Analyses of the spectral profile in the shorter time window (T1) showed three spectroscopically distinct species (Figure 2B). The concentration of one of the species decreases with time, and it was assigned as the apoprotein (species A[HS]) characterized by no absorption peaks in the visible region. The first intermediate species that initially exhibits an increase in concentration with time (Figure 2C) and subsequently a decrease with a further increase in time was characterized by an intense peak at ∼370 nm. This species is labeled as intermediate X. The second intermediate characterized by an intense band at ∼455 nm (Figure 2B) exhibits an increase in concentration with time in the shorter time window (T1) and is labeled species Y. The concentration of the same species Y (with an absorption band at ∼455 nm) that increased in the shorter time window (T1) was found to decrease in the longer time window (T2) with concomitant formation of the holoprotein (species H) as shown in the insets of panels B and C of Figure 2. It is important to note that we could derive the spectra of X and Y only in the visible region (340−690 nm) in the stopped-flow diode array system and the absorption peaks of both of these species are quite broad. Hence, each of the species X and Y could also exist as a mixture of species with visible absorption bands that are close together. It is important to note that the experiments were conducted under pseudo-first-order conditions using $Cu(His)_2$ at high concentrations, which do not change effectively during the reaction.

The UV−visible spectral features of species X agree with the "early intermediate" reported recently,[15] which was proposed to include coordination of a sulfur (Cys) ligand to the copper ion ([N2S]-type coordination).[21,22,24] Such an intermediate species was also reported during incorporation of the metal ion into the Se(Met)160 mutant of $TtCu_A$ at ambient pH,[15] the nitrous oxide reductase (N_2OR),[19] and the purple Cu_A-azurin[18,20] and was assigned as a "red copper" center of a mononuclear cupric thiolato species coordinated in a distorted tetragonal geometry.[23,25,37,38]

The spectrum of species Y matches that of the "green intermediate" with an absorption maximum at ∼455 nm reported recently[15] that was proposed to include coordination of sulfur (Cys and Met) and nitrogen (His) ligands [S2N] to copper ion with a strong interaction between the (Cys)S p(σ) orbital and the Cu $d_{x^2-y^2}$ orbital, giving rise to the intense S−Cu charge transfer transition band.[15,39,40]

The kinetics of the reaction of the apoprotein of $TtCu_A$ with $Cu(His)_2$ was also studied at pH 5 and 6 (see Figure S2A,D of the Supporting Information) in the same time windows as that at pH 7 to assess the effect of pH on metal ion incorporation. The spectral profiles of the reactions were studied at the same two time windows at each pH as those at pH 7. The time evolutions of the absorption spectra upon mixing of $Cu(His)_2$

dx.doi.org/10.1021/bi400101g | Biochemistry 2013, 52, 4620−4635

Table 1. Observed Rate Constants (k_{obs}) of Species X, Y, Z, and H for the Individual Reaction Steps (defined in Scheme 1) Obtained from Optimal Fits Using Pro-K for $TtCu_A$ Assembly[a]

	rate constant (s^{-1})											
	WT $TtCu_A$			D111K $TtCu_A$			D111N $TtCu_A$			D111E $TtCu_A$		
	pH 5	pH 6	pH 7	pH 5	pH 6	pH 7	pH 5	pH 6	pH 7	pH 5	pH 6	pH 7
step 1	25.7 ± 1.3	32.3 ± 1.6	40.1 ± 2.0	16.2 ± 0.8	43.9 ± 2.2	75.2 ± 3.8	29.8 ± 1.5	43.9 ± 2.2	58.6 ± 2.9	30.5 ± 1.5	37.4 ± 1.9	52.1 ± 2.6
step 2	08.0 ± 0.4	10.4 ± 0.5	12.0 ± 0.6	–	–	03.4 ± 0.2	–	–	11.4 ± 0.6	–	–	11.2 ± 0.6
step 4	0.099 ± 0.004	0.048 ± 0.002	0.033 ± 0.002	0.468 ± 0.023	0.287 ± 0.014	0.194 ± 0.010	0.384 ± 0.019	0.322 ± 0.016	0.284 ± 0.014	0.228 ± 0.011	0.185 ± 0.009	0.113 ± 0.006

[a] A[HS] is the reduced apoprotein. H is the purple Cu_A. X, Y, and Z are intermediate species. Protein and Cu(II) concentrations were 0.18 and 1 mM, respectively.

with the apoprotein of WT $TtCu_A$ were analyzed with Pro-K, and two distinct intermediate species X and Y analogous to that observed at ambient pH were observed in the reaction mixture at pH 6 as well as at pH 5. The spectra of species X and Y derived from the SVD analyses, however, showed a distinct dependence on pH (Figure 2B and Figure S2B,E of the Supporting Information). The time evolution of the concentrations of these intermediates (X and Y), however, was similar to that observed at pH 7 (Figure S2C,F of the Supporting Information). The spectrum of the final product, H, matched that of the purple Cu_A at the different pHs reported previously.[41] Close inspection of the results of Pro-K analyses (Figure 2C and Figure S2B,E of the Supporting Information) showed that the spectra of intermediate species Y obtained in the shorter time window, T1, were slightly red-shifted in the longer time window, T2. This effect is more prominent at lower pH. This indicates that species Y might not be a unique species of the metal ion bound to the apoprotein; rather, there might be a continuous movement of the metal ion within the coordination sphere in the protein cavity. The values of the observed pseudo-first-order rate constants (k_{obs}) obtained from the analyses of the kinetic data at different pHs are shown in Table 1. The k_{obs} for the formation of X was faster than that of species Y, which is several orders of magnitude faster than that of formation of the holoprotein (H). Moreover, the k_{obs} values for X and Y were found to decrease with a decrease in pH, while the k_{obs} for the final step (in time window T2) of formation of the holoprotein (H) was increased with a decrease in pH.

Kinetics of Incorporation of Copper Ion into the D111AA (AA = K, N, or E) Mutant Apoprotein of $TtCu_A$. Recent studies have shown that mutation of Met160 to SeMet leads to changes in the spectral properties of the intermediates formed during incorporation of the metal ion into the $TtCu_A$ apoprotein.[15] Such changes were ascribed to the changes in the axial interaction caused by the ligand substitution during the incorporation of the metal ion into the protein.[15] It, however, remains to be seen whether changes in an outer sphere residue, residing close to the coordinated residue, could affect the mechanism of incorporation of the metal ion into the active site of the protein. Analysis of the crystal structure of the protein (PDB entry 2CuA) indicates that Asp111 may be hydrogen bonded to His114 that is coordinated to one of the copper centers in the holoprotein. The kinetics of incorporation of copper ion into the apoprotein of various mutants of Asp111 was monitored in two time windows (shorter, T1, and longer, T2). The time windows were optimized separately for each mutant, and the same set of time windows was used for a given mutant at different pHs.

The apoproteins of all the three mutants, D111K, D111N, and D111E, of $TtCu_A$ showed formation of the early intermediate (Figure 3A and Figures S4A and S5A of the Supporting Information for D111K, D111N, and D111E, respectively) upon addition of $Cu(His)_2$ with a distinct absorption maximum at ~370 nm at ambient pH similar to that observed in the case of the WT species. The time windows selected for the kinetic studies were 0−1.2 s (T1) for D111K, 0−0.6 s (T1) for D111N, and 0−1.2 s (T1) for D111E and 0−60 s (T2) for D111K and D111N and 0−130 s (T2) for D111E. Analogous to the that of the WT protein, SVD analyses of the results using Pro-K showed that apart from the early intermediate, all three mutants give one more intermediate species in the shorter time window (T1). The UV−visible

dx.doi.org/10.1021/bi400101g | Biochemistry 2013, 52, 4620−4635

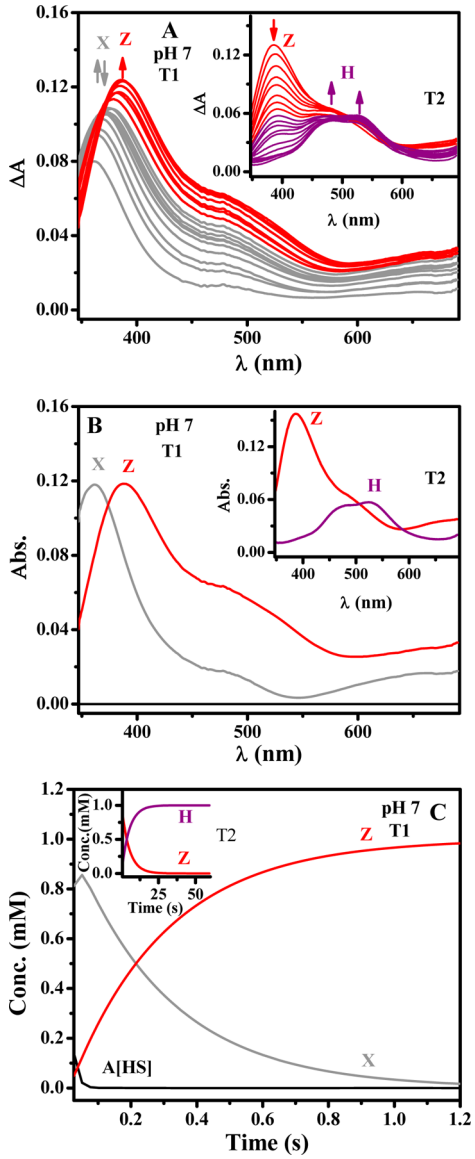

Figure 3. Stopped-flow UV−visible absorbance spectra, resolved species spectra, and corresponding concentration profiles obtained from global analysis after 5.6 equiv of $Cu(His)_2$ had been mixed with the apoprotein of D111K $TtCu_A$ over T1 and T2 (inset) at pH 7 (A−C) in UB under aerobic conditions. The constant temperature of 15 °C was maintained during the course of reaction. The first spectrum was collected at 13.7 ms and 1.3 s (inset). Spectra are colored to correspond to the species forming in that particular time frame. Arrows indicate the direction of the change in absorbance during the course of experiment and are colored to correspond to the species forming in that time interval. A[HS] is the reduced apoprotein. H is the purple Cu_A. X and Z are intermediate species.

absorption spectrum of the second intermediate showed a distinct band at ∼390 nm at ambient pH (Figure 3B and Figures S4B and S5B of the Supporting Information for D111K, D111N, and D111E, respectively). This species observed at pH 7 is labeled species Z. The results in the longer time window (T2) showed that species Z is directly converted to the holoprotein (H) and any intermediate similar to species Y observed in the case of the WT protein was not detected in the case of the mutants. Analyses of the time evolution of the concentrations of each of the species showed that the level of the early intermediate (X) initially increases with time in time window T1, reaches a maximum, and then decays like that observed in the case of the WT protein. The concentration of species Z increases with time in time window T1 and subsequently decreases in the longer time window (T2), giving rise to the formation of the holoprotein (Figure 3C and Figures S4C and S5C of the Supporting Information).

The kinetics of incorporation of the metal ion into the apoprotein of the D111AA (AA = K, N, or E) mutants of $TtCu_A$ was also studied at pH 5 and 6 in the same time windows as those at pH 7 (Figures S3A,D, S4D,G, and S5D,G of the Supporting Information). The SVD analyses of the spectral changes (Figures S3B,E, S4E,H, and S5E,H of the Supporting Information) with time gave three components in the faster time window (T1) at both pHs for all the mutants. The results in the longer time window (T2) could be analyzed by two components at pH 6, while it gave only one component at pH 5 for all three mutants (Figures S3B,E, S4E,H, and S5E,H of the Supporting Information). Analogous to the WT protein, the early intermediate (X) detected at pH 6 and 5 was characterized by a sharp absorption band at ∼370 nm, which was pH-dependent. However, unlike the WT protein, the second intermediate species detected in time window T1 in the case of the mutants were distinctly different at the three pHs studied. The second intermediate formed at pH 6 was characterized by a sharp absorption band at ∼380 nm and labeled as species W (Figures S3B, S4E, and S5E of the Supporting Information for the D111K, D111N, and D111E mutants, respectively). This species is slightly blue-shifted compared to that obtained at pH 7 (species Z). Analogous to that of species Z (at pH 7), the concentration of species W (at pH 6) also increases with time in time window T1 and decreases with time in the longer time window (T2) forming the holoprotein (H) as shown in Figures S3C, S4F, and S5F of the Supporting Information for the D111K, D111N, and D111E mutants, respectively. The second species (species V) detected in the shorter time window (T1) in the analysis of the kinetic data at pH 5 for the mutants (Figures S3E, S4H, and S5H of the Supporting Information for the D111K, D111N, and D111E mutants, respectively) was distinctly different from that observed at pH 7 (species Z) and pH 6 (species W). This species (V) was characterized by absorption bands at ∼385, ∼480, and ∼530 nm, and the concentration of this species was found to increase with time in time window T1 in the case of all mutants at pH 5. However, this species transforms into the holoprotein (H) on the longer time scale (T2), and only one species (holoprotein, H) was observed in the longer time window at pH 5 for all the mutants (Figures S3F, S4I, and S5I of the Supporting Information for the D111K, D111N, and D111E mutants, respectively). The analyses of the kinetic data by Pro-K showed that the values of k_{obs} for the formation of species X were much larger in the case of the mutants than in the case of the WT protein (Table 1). On the other hand, the values of k_{obs} for the formation of the second intermediate (Z, W, or V) observed in the shorter time window (T1) were smaller than that of the WT protein, and a decrease in pH decreased the values of k_{obs} obtained in the shorter time window as observed in the case of the WT protein. The rates of formation of the holoprotein (H) in the final step of the reaction (in time window T2) in the case of all three mutants were orders of magnitude faster than that in the case of the WT protein (Table 1). Moreover, the values of k_{obs} for the formation of the holoprotein (H) obtained in the longer time window (T2) were found to increase with a decrease in pH.

dx.doi.org/10.1021/bi400101g | *Biochemistry* 2013, 52, 4620−4635

It is important to note that the UV−visible spectra of the intermediate species (X, Y, Z, W, or V) derived from the SVD analyses of the diode array kinetic results may not correspond to any pure species, and the possibility of the presence of a mixture of species cannot be ruled out in these cases by the studies presented here as reported previously for azurin.[24] Spectroscopic features of the early intermediate (X) and the second intermediate (Y) of the WT protein match with those reported previously.[15] The UV−visible spectral signatures of the Z and W intermediates formed at pH 7 and 6, respectively, for the mutant proteins resemble those of the red copper center of nitrosocyanin (from *Nitrosomonas europeana*, PDB entry 1IBY), which is proposed to be coordinated to two His residues, one Cys, one water, and a single side chain oxygen of Glu in a pseudo-square pyramidal geometry.[25,26,37] Another report of a red copper center was found in Sco protein (PDB entry 2B7J) coordinated to one His and two Cys residues in a tetragonally distorted environment.[15,23,42] The mutation of the D111 residue in this case possibly disfavors the formation of the coordination geometry of intermediate species Y because of the perturbation in ligand field strength, and intermediates Z, W, and V were observed during the incorporation of metal ion into the mutant proteins (D111AA). Analogous variations in the pathway of metal ion incorporation were reported previously in the case of azurin and nitrite reductase.[38,43] A red copper center was detected upon replacement of the coordinated Met with homocysteine instead of a blue copper center in the mutant azurin.[38] Mutation of the axial Met to Thr in nitrite reductase analogously led to a blue copper center in the mutant instead of the green copper in the WT nitrite reductase.[43] On the basis of the structures of the Sco protein and that of nitrosocyanin, the second intermediate (Z, W, or V species) in the case of the D111AA mutants indicates the possibility of coordination of either two His residues and one Cys ([N2S] coordination) or two Cys residues and one His ([S2N] coordination) to the copper center.

The results indicate that species X is possibly coordinated to sulfur (Cys) from the protein and free His from $Cu(His)_2$. The conversion of intermediate species X to species Y (in the WT protein) or Z, W, and V (in different D111 mutants) possibly involves coordination of the His residue from the protein matrix with different degrees of distortion in the coordination geometry of the copper ion. This distortion possibly is responsible for the formation of different absorption spectra of species Y, Z, W, and V. Intermediate species X is short-lived in both WT and D111AA variants of $TtCu_A$, but the metal binding site could self-stabilize via a rearrangement to bind a His residue of the protein and generate intermediate species Y, Z, W, or V from early intermediate X. The mononuclear Cu(II) was earlier reported to be stabilized via His residue coordination in BsSco, and mutation of the His to either Ala or Met was shown to result in autoreduction of Cu(II) and subsequent oxidation of the two thiolates to a disulfide bond.[44]

EPR Spectroscopy. To gain further insight into the coordination geometry of the copper ion in the intermediate species during incorporation of copper ions into the apoprotein matrix, the EPR spectrum of intermediate species Y was recorded at ambient pH (pH 7) and 93.7 K. A substoichiometric concentration of $Cu(His)_2$ (0.4 equiv) was used to reduce the magnitude of the background signal of free $Cu(His)_2$. The reaction mixture collected within the time period of 250 ms contained species Y, which was ensured by the stopped-flow UV−visible diode array measurement (Figure 2C). The EPR spectrum (Figure S10 of the Supporting Information) of the 250 ms reaction mixture containing the intermediate species (Y) at ambient pH was found to have overlapping hyperfine shifted peaks in the low field region, indicating presence of a mixture of at least two nonequivalent Cu(II) species. The spectra in the 2500−3100 G region could be fit as a sum of two sets of four Gaussian functions (total of eight Gaussians), indicating the presence of two mononuclear copper(II) species with different g_z and hyperfine coupling constant (A_z) values. The simulation of the z component of the EPR spectrum is shown in the inset of Figure S10 of the Supporting Information showing each set of four Gaussians separately. Each of these Gaussians corresponds to hyperfine splitting for one Cu(II) center, suggesting that there are possibly two types of copper centers in the mixture. These two copper centers were found to have g_z values of 2.353 and 2.278, with corresponding hyperfine coupling constants (A_z) of 144.2 and 169 G, respectively (Figure S10 of the Supporting Information). The EPR spectrum of $Cu(His)_2$ shown in the bottom panel of Figure S10 of the Supporting Information gave g_z and A_z values of 2.278 and 169 G, respectively (Table S3 of the Supporting Information), which agree with those from an earlier report.[45] Via comparison of the EPR spectra of the reaction mixture and that of pure $Cu(His)_2$ (Table S3 of the Supporting Information), the EPR parameters of intermediate species Y were derived to be 2.353 (g_z) and 144.2 G (A_z) (Figure S10 of the Supporting Information). The EPR parameters for the second intermediate (species Z) from the D111K mutant estimated from the analyses of the spectrum of the freeze quenched reaction mixture of the mutant of $TtCu_A$ were found to be (g_z = 2.336, and A_z = 158 G) slightly larger than those derived for the green intermediate (species Y) of the WT protein (Table S3 of the Supporting Information). The g_z as well as A_z values for the red Cu (from BsSco and from nitrosocyanin) are reported to be higher than those for the green Cu intermediate observed in the M160SeM mutant of $TtCu_A$.[25,42,46−51] The A_z value of the green Cu species obtained from the M160SeM mutant of $TtCu_A$ was reported to be 116 G, which is slightly smaller than that of the intermediate species (Y) obtained from WT $TtCu_A$ in this case.[15] This is possibly due to the strong interaction between sulfur and copper ion compared to that between Se and copper ion, leading to a larger splitting of energy states and a higher A_z value in intermediate Y obtained from the WT protein.[52] The A_z of intermediate species Z from the D111K mutant is comparable to that of the red copper site of BsSco and nitrosocyanin (Table S3 of the Supporting Information).

Order of the Reaction and Determination of k_{off} and k_{on}. The kinetics of copper ion incorporation was studied at different concentrations of $Cu(His)_2$ at 15 °C at different pHs for WT $TtCu_A$ as well as for D111AA (AA = K, N, or E) mutants of the protein. Global analyses of the time-dependent spectra showed the presence of three distinct steps (Scheme 1) of the reaction at all pH values, and the k_{obs} values for each step were evaluated. The values of k_{obs} increased linearly with copper concentration for each of these steps (Figure 4 and Figures S6−S8 of the Supporting Information). The off rate constant (k_{off}) was estimated from the intercept of the plot of k_{obs} versus metal ion concentration associated with each step. The values of k_{off} are listed in Table 2, which shows that the k_{off} values increase with an increase in pH for species X, Y, and Z but decrease for the purple Cu_A (H), which is possibly due to the formation of a rigid Cu_2S_2 diamond core in the latter.

dx.doi.org/10.1021/bi400101g | *Biochemistry* 2013, 52, 4620−4635

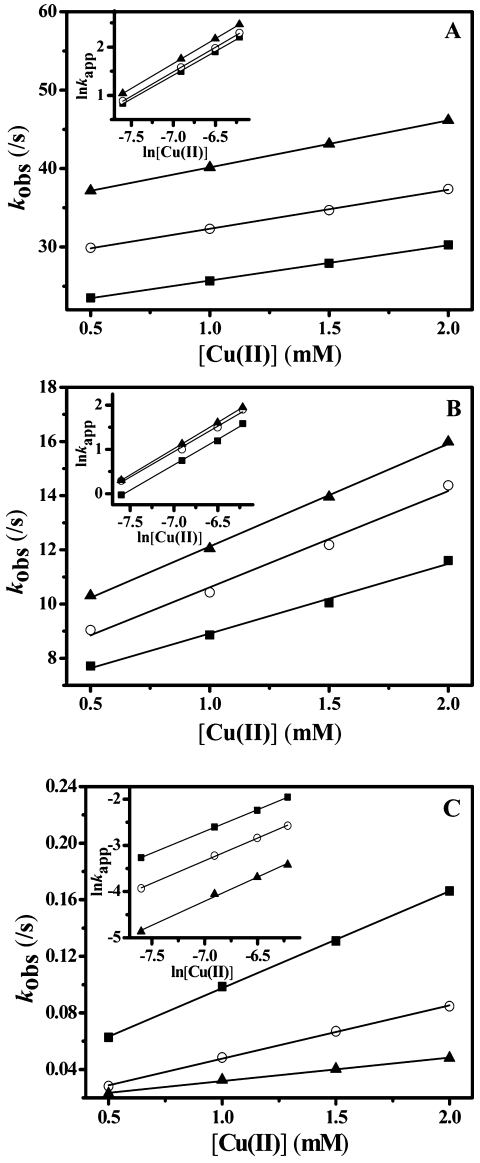

Figure 4. Plot of k_{obs} as a function of copper ion concentration and ln k_{app} vs ln[Cu(II)] (inset) for (A) intermediate species X, (B) intermediate species Y, and (C) purple Cu_A (H) of WT $TtCu_A$ at 15 °C and pH 5 (■), 6 (○), and 7 (▲).

The apparent forward rate constant (k_{app}) at each copper ion concentration in a given step of the reaction was calculated from the difference in the k_{obs} and k_{off} values associated with the step (Scheme 1). To determine the order (n) of the reaction with respect to copper ion, ln(k_{app}) was plotted versus ln[Cu(II)] for each step of the reaction (intercepts of Figure 4 and Figures S6−S8 of the Supporting Information), which fit to linear equation (eq 7)

$$k_{obs} = k_{off} + k_{on}[Cu^{2+}]^n$$

$$k_{app} = k_{obs} - k_{off} = k_{on}[Cu^{2+}]^n$$

$$\ln(k_{app}) = \ln(k_{on}) + n \times \ln[Cu^{2+}] \quad (7)$$

Analyses of the results show that the order of each reaction step was one (i.e., $n = 1 \pm 0.05$), which supports Scheme 1.

Scheme 1 shows that apo-$TtCu_A$ binds the first copper ion in a first-order reaction (step 1) to produce early intermediate

Table 2. Off Rate Constants (k_{off}) of Species X, Y, Z, and H for the Individual Reaction Steps (defined in Scheme 1) for $TtCu_A$ Assembly[a]

	rate constant (s^{-1})											
	WT $TtCu_A$			D111K $TtCu_A$			D111N $TtCu_A$			D111E $TtCu_A$		
	pH 5	pH 6	pH 7	pH 5	pH 6	pH 7	pH 5	pH 6	pH 7	pH 5	pH 6	pH 7
step 1	21.2 ± 1.1	27.5 ± 1.4	34.4 ± 1.7	2.7 ± 0.1	26.6 ± 1.3	54.9 ± 2.7	23.4 ± 1.2	36.8 ± 1.8	51.0 ± 2.6	24.4 ± 1.2	29.6 ± 1.8	41.1 ± 2.1
step 2	6.7 ± 0.3	7.7 ± 0.4	8.9 ± 0.4	–	–	2.1 ± 0.1	–	–	8.9 ± 0.4	–	–	7.6 ± 0.4
step 4	0.025 ± 0.001	0.009 ± 0.001	0.015 ± 0.001	0.161 ± 0.008	0.114 ± 0.006	0.102 ± 0.005	0.183 ± 0.009	0.134 ± 0.007	0.103 ± 0.005	0.065 ± 0.003	0.059 ± 0.003	0.031 ± 0.002

[a] A[HS] is the reduced apoprotein. H is the purple Cu_A. X, Y, and Z are intermediate species. Protein and Cu(II) concentrations are 0.18 and 1 mM, respectively.

dx.doi.org/10.1021/bi400101g | Biochemistry 2013, 52, 4620−4635

species X, which possibly consists of a mononuclear copper center with [N2S]-type coordination in a distorted tetragonal geometry as reported previously.[15] The second copper binding (step 2) to species X (resulting in formation of intermediate Y or Z) is also first-order with respect to the metal ion and possibly consists of two isolated Cu(II) centers, with either very similar coordination geometries (e.g., [S2N] or [N2S]) or one copper center behaving like $Cu(His)_2$, e.g., [N2O2]-type coordination (Figure S10 of the Supporting Information) and the other one in [S2N] (or [N2S])-type coordination.[45] The final stage of formation of the purple copper center (step 4) was found to be first-order with respect to copper ions and possibly involves reduction of one of the copper ions of the second intermediate (Y or Z). The reduction of Cu(II) to Cu(I) is a key step for the maturation of the Cu_A site, and hence, it needs to accept an electron. As no additional reducing agent was added to the reaction mixture, the reducing equivalents are possibly provided by the Cys residues of the apoprotein (A[HS]) as shown in step 3 of Scheme 1 as proposed previously.[15,18−20] The in situ-generated Cu(I) ion may either transfer an electron to the second intermediate (species Y or Z) or substitute one of the Cu(II) ions of this intermediate,[53] followed by a conformational rearrangement leading to the formation (step 4) of the purple holoprotein (H) containing a charge-delocalized dinuclear copper center at the active site.

The bimolecular rate constants (k_{on}) for each step were determined from the intercept of the plot of $\ln(k_{app})$ vs $\ln[Cu(II)]$ at each pH (inset of Figure 4 and Figures S6−S8 of the Supporting Information). The k_{on} values matched those determined from the slope of the plot of k_{app} versus [Cu(II)], confirming that the reactions were first-order with respect to copper ion concentration. The k_{on} value for the formation of species X in the case of WT $TtCu_A$ at ambient pH (pH 7) was found to be 7.2×10^3 M^{-1} s^{-1}, which agrees with that reported recently for the formation of the early intermediate[15] (Table 3). The results of Table 3 show that unlike that of the D111K mutant, the k_{on} values for the formation of species X in the case of the D111N and D111E mutants of $TtCu_A$ at a given pH are relatively closer to that in the case of the WT protein. This possibly indicates that replacement of the Asp residue with Glu or Asn at position 111 possibly does not drastically affect the conformation of the coordinating residue in the corresponding apoproteins at a given pH, while the conformation of at least some of the coordinating residues (e.g., His114) might be altered in the apoprotein of the D111K mutant compared to that in the WT protein.

The results further show that the k_{on} values for step 1 and step 2 of the reaction (Scheme 1) decrease with a decrease in pH for the WT as well as for all three mutants of $TtCu_A$. This is possibly due to the increased stability of the protonated forms of the coordinating ligands at lower pHs. The k_{on} value for the formation of the second intermediate species Y in the case of the WT protein is 1 order of magnitude larger than that for species Z that was detected in the case of the D111AA (AA = K, N, or E) mutants at ambient pH (Table 3). The k_{on} values for the final step of the reaction (step 4) forming the purple Cu_A (H) were found to increase with a decrease in pH for the WT and all three mutants (Table 3). Because step 4 involves a redox reaction between Cu(I) and the early intermediate (species Y or Z) as proposed in Scheme 1, the kinetics of this step possibly is related to the redox potentials of the two components of the reaction.[54] The results indicate that the

Table 3. Bimolecular Rate Constants (k_{on}) of Species X, Y, Z, and H for the Individual Reaction Steps (defined in Scheme 1) for $TtCu_A$ Assembly[a]

	rate constant ($\times 10^3$ M^{-1} s^{-1})											
	WT $TtCu_A$			D111K $TtCu_A$			D111N $TtCu_A$			D111E $TtCu_A$		
	pH 5	pH 6	pH 7	pH 5	pH 6	pH 7	pH 5	pH 6	pH 7	pH 5	pH 6	pH 7
step 1	4.1 ± 0.2	4.5 ± 0.2	7.2 ± 0.4	11.5 ± 0.6	14.3 ± 0.7	17.1 ± 0.9	5.0 ± 0.3	7.3 ± 0.4	10.0 ± 0.5	6.3 ± 0.3	8.1 ± 0.4	9.1 ± 0.5
step 2	6.0 ± 0.3	8.1 ± 0.4	11.5 ± 0.6	–	–	0.64 ± 0.03	–	–	2.4 ± 0.1	–	–	2.5 ± 0.1
step 3			(7.5 ± 1.1)[b]			(3 ± 0.31)[b]						
step 4	0.049 ± 0.002	0.034 ± 0.002	0.022 ± 0.001	0.500 ± 0.030	0.238 ± 0.010	0.135 ± 0.007	0.191 ± 0.010	0.164 ± 0.008	0.143 ± 0.007	0.158 ± 0.008	0.107 ± 0.005	0.081 ± 0.004

[a]A[HS] is the reduced apoprotein. H is the purple Cu_A. X, Y, and Z are intermediate species. Protein and Cu(II) concentrations are 0.18 and 1 mM, respectively. [b]Taken from ref 15.

dx.doi.org/10.1021/bi400101g | Biochemistry 2013, 52, 4620−4635

redox potential of the early intermediate possibly increases more sharply with a decrease in pH compared to that of the Cu(I) formed by step 3. However, the kinetic factors (e.g., reorganization energy) influencing the electron transfer kinetics at low pH may also be important in this case.

It is important to note that the formation of intramolecular (as well as intermolecular) disulfide bonds by oxidation of the apoproteins (dithiol form) would disfavor binding of the metal ion at the active site and thus would not allow the formation of the purple Cu_A species. To assess the extent of the disulfide form of the apoprotein in the reaction solution, free thiols were estimated in the apoproteins of the WT and D111AA mutants. The formation of 2-nitro-5-thiobenzoic acid (TNB) upon reduction of 5,5′-dithiobis(2-nitrobenzoic acid) (DTNB) estimated from the absorbance at 412 nm[30,31] in the presence of the apoproteins of the WT and D111AA mutants (~3 μM) at pH 7 was used to determine the concentration of the free thiols in the apoprotein. Considering that each molecule of the apoprotein consists of two cysteine residues, the concentration of the apoprotein containing free thiols was estimated. The results indicated that ~80% of the apoproteins in the solution contained free thiols (i.e., disulfide-reduced form) in the case of both the WT and the mutants; i.e., ~2.5 μM apoprotein contained free thiols before the addition of $Cu(His)_2$ in this case. Because the rate constants of metal ion incorporation determined under pseudo-first-order conditions [i.e., high concentration of $Cu(His)_2$] were independent of the initial concentration of the apoprotein, the presence of ~20% unreactive form of the apoprotein did not actually affect the kinetics of the reaction.

The concentration of the holoprotein formed at the end of the reaction was estimated from the absorbance of the reaction mixture at 480 and 530 nm at the end of the kinetic experiment (after >2 h). The reaction of ~2.5 μM apoprotein (free dithiol form) at the end of the reaction with $Cu(His)_2$ was found to form ~1.2 μM purple Cu_A (holoprotein). Thus, ~1.3 μM apoprotein did not form the holoprotein, possibly because of formation of the disulfide form. The formation of Cu(I) in step 3 of Scheme 1 takes place by reaction of Cu(II) with half equivalents of the apoprotein forming the disulfide form of the apoprotein. The formation of ~1.2 μM holoprotein in the final step of the reaction (Scheme 1) would require an equal concentration (~1.2 μM) of Cu(I) consuming ~0.6 μM apoprotein (forming the disulfide form). The results thus indicate that an additional ~0.7 μM apoprotein was oxidized possibly by excess $Cu(His)_2$ or by areal oxygen during the course of the reaction. Because the estimation of the thiols and the final yield of the holoprotein were almost the same in the case of the apoproteins of the WT and the mutants of $TtCu_A$, the reaction of the apoprotein forming the disulfide form possibly exhibited no effect of the mutation of the Asp111 residue.

Activation Parameters of Incorporation of Copper Ion into the Apoproteins. The relative energy level diagrams for the various steps of the reaction were derived from the analyses of the temperature dependence of the rate constants of incorporation of metal ion into the apoprotein of WT and D111AA (AA = K, N, or E) mutants of $TtCu_A$ at pH 7. The structure of the apoprotein of this thermostable protein remains unchanged in the temperature range of this study (10−30 °C) (Table S4 of the Supporting Information). The temperature dependence of the rate constants (k_{on} and k_{off}) follows the Arrhenius equation (eq 2) for each of the steps (Scheme 1) of the copper incorporation kinetics. The plots of ln k_{on} versus $1/T$ for each step of the reaction of the WT as well as of the mutants were linear (T = 283−303 K), and the activation energies associated with the steps were determined from the slopes of the plots shown in Figure 5. The results of the analyses are shown in Figure 6 and Table S1 of the Supporting Information. The data were also analyzed using the Eyring equation (eq 3) to determine the enthalpy ($\Delta H^{\ddagger}$) of activation from the slope and entropy ($\Delta S^{\ddagger}$) of activation from the intercept of the plot of the results using eq 3 (Figure S9 of the Supporting Information). The values of the enthalpy of activation, entropy of activation, and free energy of activation ($\Delta G^{\ddagger}$ at 298 K) for each step (Scheme 1) are listed in Table S1 of the Supporting Information.

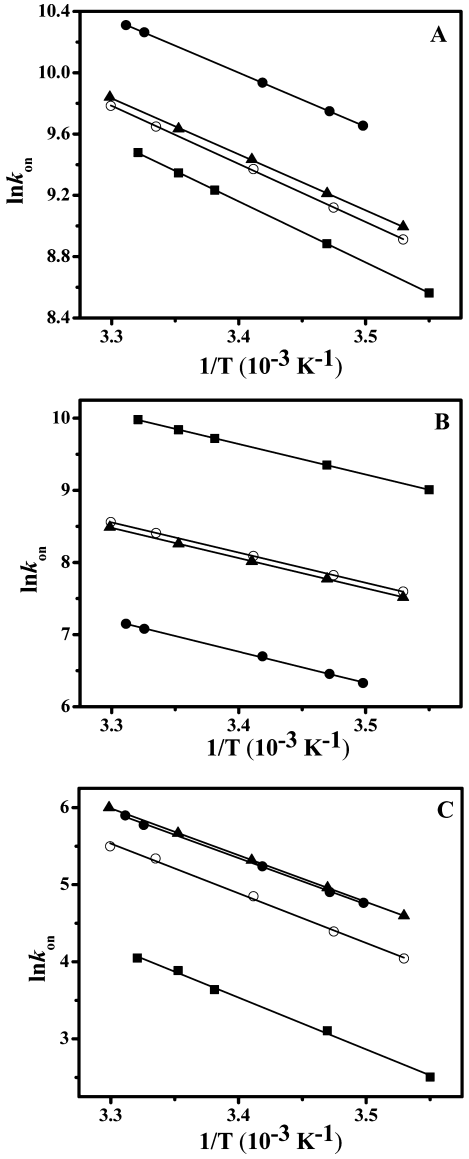

Figure 5. Plot of the Arrhenius equation (eq 2) to obtain the energy of activation for the incorporation of copper into Cu_A at pH 7. The logarithm of k_{on} is plotted as a function of reciprocal temperature: (A) intermediate species X for WT (■), D111K (●), D111N (▲), and D111E (○), (B) intermediate species Y and Z for WT (■), D111K (●), D111N (▲), and D111E (○), and (C) purple Cu_A (H) for WT (■), D111K (●), D111N (▲), and D111E (○).

dx.doi.org/10.1021/bi400101g | *Biochemistry* 2013, 52, 4620−4635

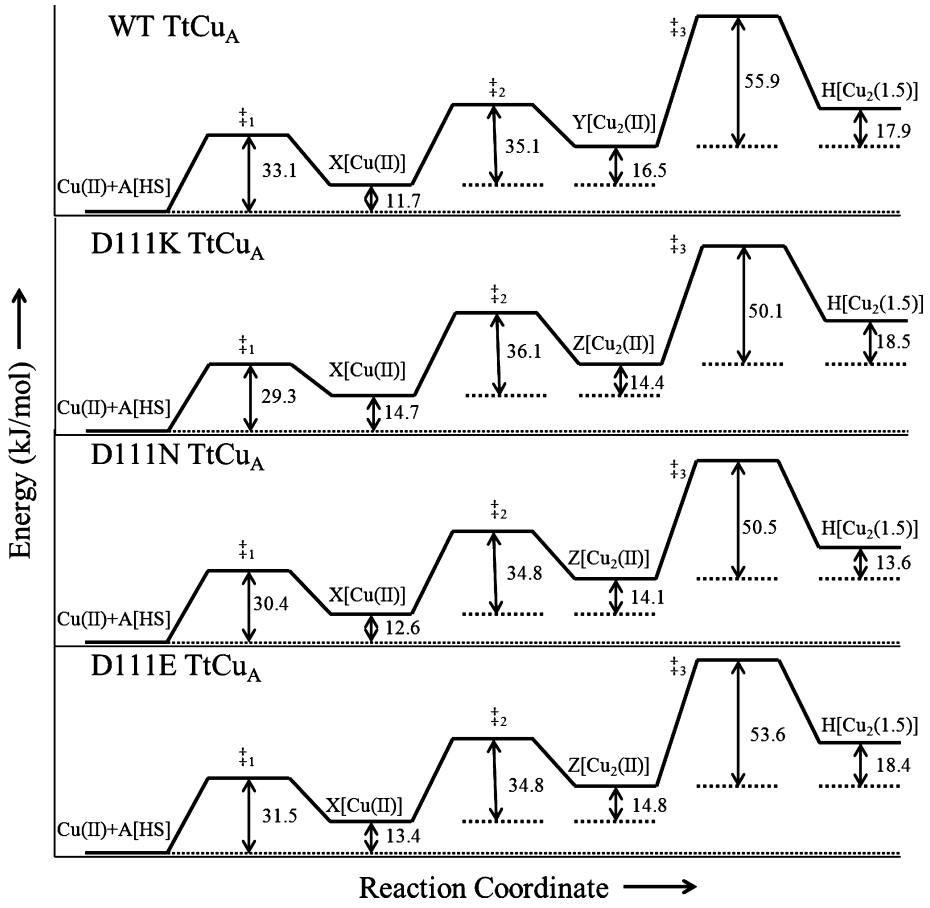

Figure 6. Schematic energy level diagram of intermediate species X, intermediate species Y or Z, and purple Cu_A (H). A[HS] is the reduced apoprotein. The ‡ notation refers to the transition state.

The activation energy (E_a) for the formation of early intermediate species X (Figure 5A) at ambient pH (pH 7) for the WT protein was found to be slightly higher (Figure 6 and Table S1 in the Supporting Information) compared to those for the three mutant proteins [$\Delta E_a = E_a(\text{WT}) - E_a(\text{D111K}) = 3.8$ kJ/mol, $\Delta E_a = E_a(\text{WT}) - E_a(\text{D111N}) = 2.7$ kJ/mol, and $\Delta E_a = E_a(\text{WT}) - E_a(\text{D111E}) = 1.6$ kJ/mol]. Analogously, the $\Delta H^‡$ values (Table S1 of the Supporting Information) for species X are slightly higher for the WT protein than for the three mutant proteins [$\Delta\Delta H^‡ = \Delta H^‡(\text{WT}) - \Delta H^‡(\text{D111AA}) = 3.8$ kJ/mol for D111K, 2.8 kJ/mol for D111N, and 1.6 kJ/mol for D111E]. On the other hand, the magnitude of $\Delta S^‡$ for species X is found to be slightly higher for the WT than for the mutants [$\Delta\Delta S^‡ = \Delta S^‡(\text{WT}) - \Delta S^‡(\text{D111AA}) = -6.1$ J mol^{-1} K^{-1} for D111K, −6.9 J mol^{-1} K^{-1} for D111N, and −3.5 J mol^{-1} K^{-1} for D111E]. The free energy of activation ($\Delta G^‡$) for the formation of the early intermediate in step 1 of the reaction (Scheme 1) at ambient pH was also found to be only slightly affected upon mutation of the D111 residue in the protein (Table S1 of the Supporting Information). This indicates that formation of the early intermediate (X) as proposed in step 1 of Scheme 1 possibly does not involve His114 in the L2 loop that is proposed (Figure 1) to be hydrogen bonded to the Asp111 residue in the protein.

The activation energies (E_a) for the formation of the second intermediate [species Y for the WT and species Z for the D111AA (AA = K, N, or E) mutants] were found to remain almost unchanged upon mutation of Asp111 (Table S1 of the Supporting Information). The $\Delta H^‡$ values for the formation of the second intermediate were also found to be very little affected by the mutation of the Asp111 residue (Table S1 of the Supporting Information). However, the $\Delta S^‡$ values were found to decrease upon mutation of Asp111 of the protein [$\Delta\Delta S^‡ = \Delta S^‡(\text{WT}) - \Delta S^‡(\text{D111AA}) = -20.6$ J mol^{-1} K^{-1} for D111K, −14.3 J mol^{-1} K^{-1} for D111N, and −13.7 J mol^{-1} K^{-1} for D111E]. The entropy effect is strongest in the case of the D111K mutant, indicating that the introduction of a positively charged residue (Lys) in place of a negative residue (Asp) possibly causes a subtle change in the conformational dynamics of the L2 loop at step 2 (Scheme 1) of the reaction. The free energies of activation ($\Delta G^‡$) for step 2 of the reaction (Scheme 1) at 298 K were found to increase in the case of the mutants compared to that in the case of the WT protein (Table S1 of the Supporting Information). Moreover, E_a, $\Delta H^‡$, and $\Delta S^‡$ for steps 1 and 2 are similar to each other, indicating that the binding of the copper ion in each of these steps possibly involves similar processes. Thus, the formation of the second intermediate (Y in WT or Z in the case of the mutants) as proposed in step 2 of Scheme 1 may not directly involve coordination of the His114 residue in the L2 loop, but there may be certain changes in conformation possibly involving the L2 loop to bring His114 closer to the metal binding site, which may affect the entropy of activation and thereby the free energy of activation for the formation of this intermediate species. It is also important to emphasize that the second intermediate (Z) in the case of the mutants at ambient pH is spectroscopically different from that formed in the case of the WT protein, suggesting that the pathway for copper ion incorporation after the formation of the first intermediate (X) may be different in the WT and the mutants.

dx.doi.org/10.1021/bi400101g | *Biochemistry* 2013, 52, 4620−4635

The activation energy (E_a) for the final step (step 4) of the reaction, i.e., formation of the purple dinuclear Cu_A (H) from the second intermediate (Y for WT or Z for mutants), slightly decreased in the case of the mutants compared to that in the case of the WT protein (Table S1 of the Supporting Information). The enthalpy of activation ($\Delta H^{\ddagger}$) associated with this step (step 4 of Scheme 1) also decreased slightly upon mutation. The values of the entropy of activation ($\Delta S^{\ddagger}$), however, showed relatively less variation upon mutation in this step of the reaction, indicating that there is possibly no major conformational change in the L2 loop containing Asp111 in this step of the reaction, though this step may involve coordination of a copper ion with His114 that interacts with the Asp111 residue. It is important to note that both the E_a and the $\Delta H^{\ddagger}$ associated with step 4 of the reaction (Scheme 1) are significantly higher compared to those of step 1 and step 2, which indicates that this step possibly involves coordination of ligands from the protein matrix and also formation of metal−metal bonds at the final step of the reaction. The entropy of activation ($\Delta S^{\ddagger}$) associated with this step is much higher in this step for all the mutants compared to those in the other two steps of the reaction. This possibly indicates that this step involves drastic conformational changes in the protein. These changes in the entropy of activation possibly arise because of changes in the solvent structure near the active site of the protein matrix. The changes in the activation parameters for step 4 of the incorporation of copper ions into the apoprotein of $TtCu_A$ possibly arise because of changes in the coordination of copper ions to the residues in the protein matrix leading to the formation of the binuclear Cu_A center.

The mechanistic details derived from the kinetic studies of incorporation of copper ion from $Cu(His)_2$ into the apoprotein of the WT and mutants of $TtCu_A$ provide some important insights that may be pertinent to the *in vivo* mechanism of maturation of the Cu_A center in cytochrome *c* oxidase. The first step of the reaction (Scheme 1) is likely to involve ligand exchange from $Cu(His)_2$ to certain surface residues near the putative binding site of the metal ion in the apoprotein. The bimolecular rate constant associated with this step (step 1) corresponds to the association of the metal ion with these surface residues forming species X. Although the coordination of copper with histidine in $Cu(His)_2$ may mimic the natural partner, the absence of any specific binding site for $Cu(His)_2$ at the surface of the apoprotein possibly results in a smaller rate constant ($\sim 7.2 \times 10^3$ M^{-1} s^{-1}) for the first step of the reaction compared to that expected for the natural partner (Sco or PCu_AC), which would have a well-defined recognition site for the binding to the apoprotein. The results shown in Figure 6 and listed in Table S1 of the Supporting Information indicate that the final step of the reaction possibly involves internal rearrangement in $TtCu_A$ and may not depend on the nature of the copper ion transporter. Furthermore, as this step is significantly affected by the mutation of Asp111, the linkage of the L2 loop may be important in this step of maturation of the protein.

Dissociation Constants and Equilibrium Free Energy. The dissociation constants (K_d) for species X, Y, Z, and H associated with the individual steps of the reaction as shown in Scheme 1 were obtained from the ratio of k_{off} and k_{on} (eq 5). The equilibrium free energies (ΔG^{Eq}) for the formation of species X, Y, Z, and H were calculated from the corresponding K_d values (eq 6) (Table S1 of the Supporting Information). The total equilibrium free energies (ΔG_T^{Eq}) were obtained by addition of the ΔG^{Eq} values associated with each step for a given mutant (eq 6) (Table S2 of the Supporting Information). The ΔG_T^{Eq} values for WT, D111K, and D111E (Table S2 of the Supporting Information) varied very little with mutation (Table S2 of the Supporting Information), except in the case of the D111N mutant where the overall free energy of formation was ∼5.8 kJ/mol higher than that for the WT protein. The overall K_d values associated with binding of copper to the apoprotein of $TtCu_A$ (Table S2 of the Supporting Information) show that the Cu(II) ion indeed has a very high affinity for the apoprotein of $TtCu_A$. Earlier studies have shown that the K_d of the Cu(II) complex of the Sco protein from *B. subtilis* (BsSco) was 45×10^{-9} M.[54] The K_d for binding of Cu(II) to the apoprotein of WT $TtCu_A$ determined by using $Cu(His)_2$ as the metal ion source in this study ($\sim 8 \times 10^{-9}$ M) is lower (i.e., stronger binding) than that for BsSco determined using $CuCl_2$.[54] This possibly indicates that the thermodynamics of ligand exchange between the donor and acceptor may be important for efficient binding of the metal ion to the target protein. The overall binding affinity of Cu(II) for the apoprotein of $TtCu_A$ was also found to depend on the nature of the residue at position 111 (Table S2 of the Supporting Information), indicating that the electrostatic interaction at the L2 loop associated with His114 and Asp111 may be important for proper binding of the metal ion to the protein.

CONCLUSIONS

The spectroscopic and kinetic studies of incorporation of copper ion into the WT and D111AA (AA = K, N, or E) mutants of $TtCu_A$ showed the formation of at least two distinct intermediates. The Asp111 residue in the L2 loop of the protein interacts with His114 coordinated to one of the copper centers in the holoprotein of $TtCu_A$. The first intermediate (species X) formed during copper ion incorporation agreed with that reported recently. This intermediate was shown to be formed even in the case of the mutants, suggesting that formation of this intermediate does not involve His114 of the L2 loop of the protein. A green colored intermediate (species Y) was identified as the second intermediate during incorporation of copper ion in the case of WT $TtCu_A$. The EPR spectra of the second intermediate showed a g_z and a hyperfine coupling constant (A_z) of 2.353 and 144.2 G, respectively, indicating the presence of a tetragonally distorted Cu(II) ion as proposed previously.[15] This green intermediate (species Y), however, was not detected in the D111AA (AA = K, N, or E) mutants of the protein. The second intermediate during incorporation of the copper ion into the apoprotein of $TtCu_A$ was found to be spectroscopically distinctly different in the mutants and the WT protein. Moreover, the absorption spectra of the second intermediate in the case of the mutants were found to be different at different pHs, indicating that the formation of this species possibly depends on the conformation of the L2 loop of the protein. These results suggested that the pathway of copper ion incorporation possibly is different in the mutants and the WT protein. The incorporation of copper ion into the apoprotein of $TtCu_A$ could be analyzed using a four-step reaction scheme (Scheme 1) derived from SVD analyses of the multiwavelength kinetic data. The replacement of the single amino acid in the L2 loop (D111) was shown to have very little effect on the kinetics of the first two steps of the reaction except that in the case of the D111K mutant, indicating that electrostatic interaction at the L2 loop possibly plays a subtle role in the mechanism of incorporation of the metal ion into the protein.

The analyses of the results at different temperatures led to the determination of the activation parameters as well as the thermodynamic parameters associated with the process. The results indicate that the mutation of Asp111 affects the entropy of activation possibly involving conformational changes in the L2 loop of the protein. The results also indicated that the overall binding affinity of Cu(II) for the apoprotein of WT $TtCu_A$ depends on the nature of ligands associated with the metal ion in the donor species [e.g., $Cu(His)_2$ in this study], and also on the nature of the residues in the outer coordination sphere (e.g., residue 111 in this case) of the acceptor (apo-$TtCu_A$).

■ ASSOCIATED CONTENT

Supporting Information

Activation parameters for intermediates and final Cu_A assembly; thermodynamic parameters for complete Cu_A assembly; compilation of literature g values and hyperfine splitting constants (A) from various green and red Cu sites; compilation of secondary structural elements of apoprotein and melting temperatures (T_m); sequence alignment of forms of subunit II from various source; stopped-flow UV−visible absorption spectra, resolved species spectra, and corresponding concentration profiles obtained from global analysis of WT $TtCu_A$ at pH 6 and 5; stopped-flow UV−visible absorption spectra, resolved species spectra, and corresponding concentration profiles obtained from global analysis of D111K $TtCu_A$ at pH 6 and 5; stopped-flow UV−visible absorption spectra, resolved species spectra, and corresponding concentration profiles obtained from global analysis of D111N $TtCu_A$ at pH 7−5; stopped-flow UV−visible absorption spectra, resolved species spectra, and corresponding concentration profiles obtained from global analysis of D111E $TtCu_A$ at pH 7−5; plot of k_{obs} as a function of copper ion concentration and ln k_{app} versus ln[Cu(II)] for D111K; plot of k_{obs} as a function of copper ion concentration and ln k_{app} versus ln[Cu(II)] for D111N; plot of k_{obs} as a function of copper ion concentration and ln k_{app} versus ln[Cu(II)] for D111E; plot of the Eyring equation; EPR spectra of $Cu(His)_2$ and intermediate species Y (250 ms); far-UV CD spectra of the apoprotein; and thermal unfolding of the apoprotein of the D111K mutant. This material is available free of charge via the Internet at http://pubs.acs.org.

Accession Codes

The soluble fragment of subunit II ($TtCu_A$) of the cytochrome c oxidase from *T. thermophilus* as PDB entry 2CuA, nitrosocyanin as PDB entry 1IBY, and yeast Sco protein as PDB entry 2B7J.

■ AUTHOR INFORMATION

Corresponding Author

*E-mail: shyamal@tifr.res.in. Telephone: +9122 22782363. Fax: +9122 22804610.

Funding

The work was supported by the Tata Institute of Fundamental Research, Mumbai.

Notes

The authors declare no competing financial interest.

■ ACKNOWLEDGMENTS

We thank Prof. B. Ludwig for kindly providing the plasmid encoding $TtCu_A$. We also thank Mr. B. T. Kansara, Prof. Ranjan Das, Mr. Krishnendu Kundu, Ms. Sushma S. Gurav, and Mr. Sandeep Goyal for help.

■ ABBREVIATIONS

CcO, cytochrome c oxidase; $TtCu_A$, Cu_A protein from subunit II of *T. thermophilus*; CD, circular dichroism; EPR, electron paramagnetic resonance; SVD, singular-value decomposition; DTNB, 5,5′-dithiobis(2-nitrobenzoic acid); AA, Lys, Asn, or Glu; WT, wild type; D111K, aspartic acid 111 mutated to lysine; D111N, aspartic acid 111 mutated to asparagine; D111E, aspartic acid 111 mutated to glutamic acid; A_z, hyperfine coupling constant due to the copper nucleus; k_{off}, off rate constant; k_{on}, bimolecular on rate constant; E_a, Arrhenius energy of activation; $\Delta H^{\ddagger}$, enthalpy of activation; $\Delta S^{\ddagger}$, entropy of activation; $\Delta G^{\ddagger}$, free energy of activation; ΔG^{Eq}, equilibrium free energy at 298 K; ΔG_T^{Eq}, total equilibrium free energy at 298 K; K_d, dissociation constant at 298 K.

■ REFERENCES

(1) Chan, S. I., and Li, P. M. (1990) Cytochrome-C Oxidase: Understanding Natures Design of a Proton Pump. *Biochemistry 29*, 1−12.

(2) Tsukihara, T., Aoyama, H., Yamashita, E., Tomizaki, T., Yamaguchi, H., ShinzawaItoh, K., Nakashima, R., Yaono, R., and Yoshikawa, S. (1996) The whole structure of the 13-subunit oxidized cytochrome c oxidase at 2.8 angstrom. *Science 272*, 1136−1144.

(3) Wilmanns, M., Lappalainen, P., Kelly, M., SauerEriksson, E., and Saraste, M. (1995) Crystal structure of the membrane-exposed domain from a respiratory quinol oxidase complex with an engineered dinuclear copper center. *Proc. Natl. Acad. Sci. U.S.A. 92*, 11955−11959.

(4) Williams, P. A., Blackburn, N. J., Sanders, D., Bellamy, H., Stura, E. A., Fee, J. A., and McRee, D. E. (1999) The Cu-A domain of *Thermus thermophilus* ba_3-type cytochrome c oxidase at 1.6 angstrom resolution. *Nat. Struct. Biol. 6*, 509−516.

(5) Ostermeier, C., Harrenga, A., Ermler, U., and Michel, H. (1997) Structure at 2.7 angstrom resolution of the *Paracoccus denitrificans* two-subunit cytochrome c oxidase complexed with an antibody F-V fragment. *Proc. Natl. Acad. Sci. U.S.A. 94*, 10547−10553.

(6) Iwata, S., Ostermeier, C., Ludwig, B., and Michel, H. (1995) Structure at 2.8-Angstrom Resolution of Cytochrome *c* Oxidase from *Paracoccus denitrificans*. *Nature 376*, 660−669.

(7) Brown, K., Tegoni, M., Prudencio, M., Pereira, A. S., Besson, S., Moura, J. J., Moura, I., and Cambillau, C. (2000) A novel type of catalytic copper cluster in nitrous oxide reductase. *Nat. Struct. Biol. 7*, 191−195.

(8) Haltia, T., Brown, K., Tegoni, M., Cambillau, C., Saraste, M., Mattila, K., and Djinovic-Carugo, K. (2003) Crystal structure of nitrous oxide reductase from *Paracoccus denitrificans* at 1.6 angstrom resolution. *Biochem. J. 369*, 77−88.

(9) Saraste, M. (1999) Oxidative phosphorylation at the fin de siecle. *Science 283*, 1488−1493.

(10) Slutter, C. E., Sanders, D., Wittung, P., Malmstrom, B. G., Aasa, R., Richards, J. H., Gray, H. B., and Fee, J. A. (1996) Water-soluble, recombinant CuA-domain of the cytochrome ba3 subunit II from *Thermus thermophilus*. *Biochemistry 35*, 3387−3395.

(11) Holm, L., Saraste, M., and Wikstrom, M. (1987) Structural Models of the Redox Centers in Cytochrome-Oxidase. *EMBO J. 6*, 2819−2823.

(12) Blackburn, N. J., Ralle, M., Gomez, E., Hill, M. G., Pastuszyn, A., Sanders, D., and Fee, J. A. (1999) Selenomethionine-substituted *Thermus thermophilus* cytochrome ba3: Characterization of the Cu-A site by Se and CuK-EXAFS. *Biochemistry 38*, 7075−7084.

(13) Soulimane, T., Buse, G., Bourenkov, G. P., Bartunik, H. D., Huber, R., and Than, M. E. (2000) Structure and mechanism of the aberrant ba_3-cytochrome c oxidase from *Thermus thermophilus*. *EMBO J. 19*, 1766−1776.

(14) Siluvai, G. S., Nakano, M., Mayfield, M., and Blackburn, N. J. (2011) The essential role of the Cu(II) state of Sco in the maturation of the Cu-A center of cytochrome oxidase: Evidence from H135Met and H135SeM variants of the *Bacillus subtilis* Sco. *J. Biol. Inorg. Chem. 16*, 285−297.
(15) Chacon, K. N., and Blackburn, N. J. (2012) Stable Cu(II) and Cu(I) Mononuclear Intermediates in the Assembly of the CuA Center of *Thermus thermophilus* Cytochrome Oxidase. *J. Am. Chem. Soc. 134*, 16401−16412.
(16) Abriata, L. A., Banci, L., Bertini, I., Ciofi-Baffoni, S., Gkazonis, P., Spyroulias, G. A., Vila, A. J., and Wang, S. (2008) Mechanism of Cu(A) assembly. *Nat. Chem. Biol. 4*, 599−601.
(17) Banci, L., Bertini, I., Ciofi-Baffoni, S., Katsari, E., Katsaros, N., Kubicek, K., and Mangani, S. (2005) A copper(I) protein possibly involved in the assembly of Cu-A center of bacterial cytochrome c oxidase. *Proc. Natl. Acad. Sci. U.S.A. 102*, 3994−3999.
(18) Wang, X. T., Ang, M. C., and Lu, Y. (1999) Kinetics of copper incorporation into an engineered purple azurin. *J. Am. Chem. Soc. 121*, 2947−2948.
(19) Savelieff, M. G., Wilson, T. D., Elias, Y., Nilges, M. J., Garner, D. K., and Lu, Y. (2008) Experimental evidence for a link among cupredoxins: Red, blue, and purple copper transformations in nitrous oxide reductase. *Proc. Natl. Acad. Sci. U.S.A. 105*, 7919−7924.
(20) Wilson, T. D., Savelieff, M. G., Nilges, M. J., Marshall, N. M., and Lu, Y. (2011) Kinetics of Copper Incorporation into a Biosynthetic Purple Cu-A Azurin: Characterization of Red, Blue, and a New Intermediate Species. *J. Am. Chem. Soc. 133*, 20778−20792.
(21) Lu, Y., Gralla, E. B., Roe, J. A., and Valentine, J. S. (1992) Redesign of a Type-2 into a Type-1 Copper Protein: Construction and Characterization of Yeast Copper-Zinc Superoxide-Dismutase Mutants. *J. Am. Chem. Soc. 114*, 3560−3562.
(22) Lu, Y., Roe, J. A., Bender, C. J., Peisach, J., Banci, L., Bertini, I., Gralla, E. B., and Valentine, J. S. (1996) New type 2 copper-cysteinate proteins. Copper site histidine-to-cysteine mutants of yeast copper-zinc superoxide dismutase. *Inorg. Chem. 35*, 1692−1700.
(23) Siluvai, G. S., Mayfield, M., Nilges, M. J., George, S. D., and Blackburn, N. J. (2010) Anatomy of a Red Copper Center: Spectroscopic Identification and Reactivity of the Copper Centers of *Bacillus subtilis* Sco and Its Cys-to-Ala Variants. *J. Am. Chem. Soc. 132*, 5215−5226.
(24) van Amsterdam, I. M. C., Ubbink, M., van den Bosch, M., Rotsaert, F., Sanders-Loehr, J., and Canters, G. W. (2002) A new type 2 copper cysteinate azurin: Involvement of an engineered exposed cysteine in copper binding through internal rearrangement. *J. Biol. Chem. 277*, 44121−44130.
(25) Arciero, D. M., Pierce, B. S., Hendrich, M. P., and Hooper, A. B. (2002) Nitrosocyanin, a red cupredoxin-like protein from *Nitrosomonas europaea*. *Biochemistry 41*, 1703−1709.
(26) Lieberman, R. L., Arciero, D. M., Hooper, A. B., and Rosenzweig, A. C. (2001) Crystal structure of a novel red copper protein from *Nitrosomonas europaea*. *Biochemistry 40*, 5674−5681.
(27) Ghosh, M. K., Rajbongshi, J., Basumatary, D., and Mazumdar, S. (2012) Role of the Surface-Exposed Leucine 155 in the Metal Ion Binding Loop of the CuA Domain of Cytochrome c Oxidase from *Thermus thermophilus* on the Function and Stability of the Protein. *Biochemistry 51*, 2443−2452.
(28) Maneg, O., Ludwig, B., and Malatesta, F. (2003) Different interaction modes of two cytochrome-c oxidase soluble Cu-A fragments with their substrates. *J. Biol. Chem. 278*, 46734−46740.
(29) Bradford, M. M. (1976) Rapid and Sensitive Method for Quantitation of Microgram Quantities of Protein Utilizing Principle of Protein-Dye Binding. *Anal. Biochem. 72*, 248−254.
(30) Ellman, G. L. (1959) Tissue Sulfhydryl Groups. *Arch. Biochem. Biophys. 82*, 70−77.
(31) Riddles, P. W., Blakeley, R. L., and Zerner, B. (1983) Reassessment of Ellman Reagent. *Methods Enzymol. 91*, 49−60.
(32) Reed, J., and Reed, T. A. (1997) A set of constructed type spectra for the practical estimation of peptide secondary structure from circular dichroism. *Anal. Biochem. 254*, 36−40.
(33) Behera, R. K., and Mazumdar, S. (2010) Thermodynamic basis of the thermostability of CYP175A1 from *Thermus thermophilus*. *Int. J. Biol. Macromol. 46*, 412−418.
(34) Maeder, M., and Zuberbuhler, A. D. (1990) Nonlinear Least-Squares Fitting of Multivariate Absorption Data. *Anal. Chem. 62*, 2220−2224.
(35) Henry, E. R., and Hofrichter, J. (1992) Singular Value Decomposition: Application to Analysis of Experimental Data. *Methods Enzymol. 210*, 129−192.
(36) Gamelin, D. R., Randall, D. W., Hay, M. T., Houser, R. P., Mulder, T. C., Canters, G. W., de Vries, S., Tolman, W. B., Lu, Y., and Solomon, E. I. (1998) Spectroscopy of mixed-valence Cu-A-type centers: Ligand-field control of ground-state properties related to electron transfer. *J. Am. Chem. Soc. 120*, 5246−5263.
(37) Basumallick, L., Sarangi, R., George, S. D., Elmore, B., Hooper, A. B., Hedman, B., Hodgson, K. O., and Solomon, E. I. (2005) Spectroscopic and density functional studies of the red copper site in nitrosocyanin: Role of the protein in determining active site geometric and electronic structure. *J. Am. Chem. Soc. 127*, 3531−3544.
(38) Clark, K. M., Yu, Y., Marshall, N. M., Sieracki, N. A., Nilges, M. J., Blackburn, N. J., van der Donk, W. A., and Lu, Y. (2010) Transforming a Blue Copper into a Red Copper Protein: Engineering Cysteine and Homocysteine into the Axial Position of Azurin Using Site-Directed Mutagenesis and Expressed Protein Ligation. *J. Am. Chem. Soc. 132*, 10093−10101.
(39) LaCroix, L. B., Shadle, S. E., Wang, Y. N., Averill, B. A., Hedman, B., Hodgson, K. O., and Solomon, E. I. (1996) Electronic structure of the perturbed blue copper site in nitrite reductase: Spectroscopic properties, bonding, and implications for the entatic/rack state. *J. Am. Chem. Soc. 118*, 7755−7768.
(40) Ghosh, S., Xie, X. J., Dey, A., Sun, Y., Scholes, C. P., and Solomon, E. I. (2009) Thermodynamic equilibrium between blue and green copper sites and the role of the protein in controlling function. *Proc. Natl. Acad. Sci. U.S.A. 106*, 4969−4974.
(41) Sanghamitra, N. J. M., and Mazumdar, S. (2008) Conformational dynamics coupled to protonation equilibrium at the Cu-A site of *Thermus thermophilus*: Insights into the origin of thermo stability. *Biochemistry 47*, 1309−1318.
(42) Andruzzi, L., Nakano, M., Nilges, M. J., and Blackburn, N. J. (2005) Spectroscopic studies of metal binding and metal selectivity in *Bacillus subtilis* BSco, a homologue of the yeast mitochondrial protein scolp. *J. Am. Chem. Soc. 127*, 16548−16558.
(43) Basumallick, L., Szilagyi, R. K., Zhao, Y. W., Shapleigh, J. P., Scholes, C. P., and Solomon, E. I. (2003) Spectroscopic studies of the Met182Thr mutant of nitrite reductase: Role of the axial ligand in the geometric and electronic structure of blue and green copper sites. *J. Am. Chem. Soc. 125*, 14784−14792.
(44) Siluvai, G. S., Nakano, M. M., Mayfield, M., Nilges, M. J., and Blackburn, N. J. (2009) H135A Controls the Redox Activity of the Sco Copper Center. Kinetic and Spectroscopic Studies of the His135Ala Variant of *Bacillus subtilis* Sco. *Biochemistry 48*, 12133−12144.
(45) Rotilio, G., and Calabres, L. (1971) EPR Study of Cu(II) Complexes of Tridentate Amino Acids. *Arch. Biochem. Biophys. 143*, 218.
(46) Olesen, K., Veselov, A., Zhao, Y. W., Wang, Y. S., Danner, B., Scholes, C. P., and Shapleigh, J. P. (1998) Spectroscopic, kinetic, and electrochemical characterization of heterologously expressed wild-type and mutant forms of copper-containing nitrite reductase from *Rhodobacter sphaeroides* 2.4.3. *Biochemistry 37*, 6086−6094.
(47) Iwasaki, H., Noji, S., and Shidara, S. (1975) *Achromobacter cycloclastes* Nitrite Reductase: Function of Copper, Amino-Acid Composition, and ESR Spectra. *J. Biochem. 78*, 355−361.
(48) Denariaz, G., Payne, W. J., and Legall, J. (1991) The Denitrifying Nitrite Reductase of *Bacillus halodenitrificans*. *Biochim. Biophys. Acta 1056*, 225−232.
(49) Tocheva, E. I., Rosell, F. I., Mauk, A. G., and Murphy, M. E. P. (2007) Stable copper-nitrosyl formation by nitrite reductase in either oxidation state. *Biochemistry 46*, 12366−12374.

(50) Masuko, M., Iwasaki, H., Sakurai, T., Suzuki, S., and Nakahara, A. (1984) Characterization of Nitrite Reductase from a Denitrifier, *Alcaligenes* Sp Ncib-11015: A Novel Copper Protein. *J. Biochem. 96*, 447−454.
(51) Zumft, W. G., Gotzmann, D. J., and Kroneck, P. M. H. (1987) Type-1, Blue Copper Proteins Constitute a Respiratory Nitrite-Reducing System in *Pseudomonas aureofaciens*. *Eur. J. Biochem. 168*, 301−307.
(52) Frank, P., Licht, A., Tullius, T. D., Hodgson, K. O., and Pecht, I. (1985) A Selenomethionine-Containing Azurin from an Auxotroph of *Pseudomonas aeruginosa*. *J. Biol. Chem. 260*, 5518−5525.
(53) Reedijk, J. (2012) Plasticity in the copper-thioether bond: Manifestation in blue Cu proteins and in synthetic analogs. *J. Inorg. Biochem. 115*, 182−185.
(54) Imriskova-Sosova, I., Andrews, D., Yam, K., Davidson, D., Yachnin, B., and Hill, B. C. (2005) Characterization of the redox and metal binding activity of BsSco, a protein implicated in the assembly of cytochrome c oxidase. *Biochemistry 44*, 16949−16956.